the high Be/Li ratio measured in the sun (compared to the earth value) can be explained if one supposes that the sun, since its formation, has destroyed its lithium, whereas the destruction in the earth was stopped at the time of the earth's solidification. In conclusion, one may suppose that lithium has been destroyed continually (in the sun) since its formation, while for beryllium this destruction, if there is any, is very low.

Gradsztajn[4] explains the low value for B/Li ratios in the earth and meteorites on the hypothesis that boron, being more volatile than other elements, escaped at the time of the earth's solidification.

The $^{11}B/^{10}B$ ratios we find for incident α particles are somewhat lower than Gradsztajn's theoretical ones. Taking into account the lack of precision of the ratios measured in the solar system, we can conclude that the relative abundance of boron has not been altered but remains near its production ratio. This assertion excludes (n, α) reactions as a possible destruction mechanism for the elements Li, Be, and B.

IV. CONCLUSION

The abundance of the elements Li, Be, and B measured in the solar system may be explained by the following hypothesis: The Li, Be, and B produced by spallation reactions at the surface of the stars are drawn back to the base of the convective zone, where Li is destroyed by (p, α) reactions. The temperature in this region is supposed to be about 2×10^6 °K, a temperature which is sufficient to destroy lithium but not beryllium and boron. The products of the reactions are then drawn to the surface of the star, and the observable result is a strong increase of the $^7Li/^6Li$ ratio. Such a convective zone exists in all stars. For the sun, its depth is equal to about $\frac{1}{10}$ of the solar radius.

ACKNOWLEDGMENT

The authors thank Professor H. Reeves for his interest and for his helpful suggestions.

PHYSICAL REVIEW C VOLUME 1, NUMBER 2 FEBRUARY 1970

Excitation of Collective States in Light Nuclei by Inelastic Scattering of 20.3-MeV Polarized Protons*

A. G. BLAIR
Los Alamos Scientific Laboratory, University of California, Los Alamos, New Mexico 87544
AND
C. GLASHAUSSER† AND R. DE SWINIARSKI‡
Lawrence Radiation Laboratory, University of California, Berkeley, California 94720
AND
J. GOUDERGUES, R. LOMBARD, B. MAYER, AND J. THIRION
Service de Physique Nucléaire à Moyenne Enérgie, CEN-Saclay, Saclay, France
AND
P. VAGANOV
University of Leningrad, Leningrad, U.S.S.R.
(Received 25 September 1969)

Asymmetries and relative differential cross sections have been measured for elastic and inelastic scattering of 20.3-MeV polarized protons from light elements. The targets included C^{12}, O^{16}, Mg^{24}, Mg^{25}, Mg^{26}, Al^{27}, Si^{28}, and Ca^{40}. Significant differences have been observed in both the asymmetries and cross sections for transitions with a given angular momentum transfer. The shapes of the asymmetries for Al^{27} and Si^{28} show some disagreement with the weak-coupling model prediction. Coupled-channels and distorted-wave Born-approximation calculations (DWBA) have been performed for the first 2^+ and 4^+ states in Mg^{24} and Si^{28}, with several types of deformed spin-orbit potential. In principle, it should be possible with a coupled-channel analysis to distinguish between vibrational and rotational models, and between positive and negative deformations. In fact, there are differences between the predictions of these models. However, none of them gives a good account of the 2^+ and 4^+ asymmetries in Mg^{24} and Si^{28}, even when the full Thomas form of the spin-orbit potential is used. Microscopic- and macroscopic-model DWBA predictions of the 3_1^- and 5_1^- asymmetries in Ca^{40} yield fair agreement with the experimental data.

I. INTRODUCTION

MEASUREMENTS of the asymmetry in the inelastic scattering of polarized protons from medium-weight nuclei have now been reported at 18.6,[1] 20.3,[2] 30,[3] 40,[4] and 49 MeV.[5] Results for some light nuclei at several energies have also been pub-

* Work supported in part by the U.S. Atomic Energy Commission.
† Present address: Rutgers, The State University, New Brunswick, N.J.
‡ NATO-Fulbright Fellow. Permanent address: Institut des Sciences Nucléaires de Grenoble, France.

[1] C. Glashausser, R. de Swiniarski, J. Thirion, and A. D. Hill, Phys. Rev. **164**, 1437 (1967).
[2] C. Glashausser, R. de Swiniarski, J. Goudergues, R. M. Lombard, B. Mayer, and J. Thirion, Phys. Rev. **184**, 1217 (1969).
[3] D. J. Baugh, M. J. Kenny, J. Lowe, D. L. Watson, and H. Wojciechowski, Nucl. Phys. **A99**, 203 (1967).
[4] M. P. Fricke, E. E. Gross, and A. Zucker, Phys. Rev. **163**, 1113 (1967).
[5] V. E. Lewis, E. J. Burge, A. A. Rush, and D. A. Smith, Nucl. Phys. **A101**, 589 (1967).

lished.[6] Analyses of these data with the distorted-wave Born-approximation (DWBA) or coupled-channel (CC) methods have been reasonably successful for collective levels. When the distortion of the full Thomas term is included in the interaction, the DWBA predictions for 2^+ states in the Ni isotopes at 40 MeV, e.g., are very accurate.[7] Problems have appeared, however, in attempts to describe the results with a microscopic model.[1,2] In the present paper, asymmetries are presented for inelastic proton scattering at 20.3 MeV from low-lying collective states in C^{12}, O^{16}, Mg^{24}, Mg^{25}, Mg^{26}, Al^{27}, Si^{28}, and Ca^{40}. A coupled-channel analysis of the data concentrates on Mg^{24} and Si^{28}; predictions for Ca^{40} are also shown. Results from an initial DWBA analysis of some of these data have already been published.[8]

The rotational model provides a reasonably accurate description of the low-lying levels of Mg^{24} and Mg^{25}, but the neighboring nuclei in the *s-d* shell are not so well understood. A study of differential cross sections[9] for inelastic proton scattering in this region showed a marked transition between strong coupling for Mg^{25} to weak coupling for Al^{27}. Deviations from the weak-coupling description could be revealed in differences in the asymmetries for the low-lying states in Al^{27} and the first 2^+ state in Si^{28}. The variations in the shapes of the asymmetries for a given orbital angular momentum transfer (L) are, in fact, generally interesting to study, since they indicate differences either in the structure of the states involved or in their mode of excitation. Rotational and vibrational levels, e.g., may have different asymmetries. Provided the states can be simply described in terms of these macroscopic models, a coupled-channel analysis should adequately account for variations in the mode of excitation.

After a brief description of the experimental details in Sec. II, the measured asymmetries are presented and discussed in Sec. III. Parameters of the spherical optical-model potential for Mg^{24}-Si^{28} are given in Sec. IV. The results of a coupled-channel analysis of several inelastic transitions are also shown and discussed. The paper concludes with a short summary in Sec. V.

II. EXPERIMENTAL METHODS

Details of the experimental arrangements have been described in Ref. 2. About 20 nA of 20.3-MeV polarized protons could generally be obtained on target at the Saclay sector-focused cyclotron with the external ionizer and trochoidal injection system.[10] The beam polarization was normally about 75%. Eight Si(Li) detectors were used to count the scattered protons; the over-all energy resolution in the eight systems was between 100 and 150 keV. The angular resolution was $\pm 2°$. A carbon polarimeter continuously monitored the polarization of the incident beam. Two monitor counters placed above and below the beam line provided reliable normalization for relative cross-section measurements.

TABLE I. Thickness and purity of targets.

Target	Thickness (mg/cm²)	Purity (%)
Mylar	1.0	...
Mg^{24}	1.0	99.5
Mg^{25}	1.7	99.5
Mg^{26}	2.3	99.8
Al^{27}	1.4	natural
Si^{28}	3.7	natural
Ca^{40}	1.0	natural

The purity and thickness of the targets used are listed in Table I. The magnesium targets were obtained from the Oak Ridge National Laboratory; the silicon and calcium targets were evaporated at the Saclay Laboratory. A Mylar target was used for the carbon and oxygen measurements.

III. RESULTS

The measured differential asymmetries for many low-lying excited states in the nuclei studied in the present experiment are shown in Figs. 1–9. The cross sections for a few states are shown in later figures, but they are generally not illustrated since most are already available[9] at 17.5 MeV. The asymmetry is normalized to 100% beam polarization and is defined as follows:

$$A = P_B^{-1}(N_+ - N_-)/(N_+ + N_-).$$

The quantity P_B is the measured polarization of the beam; N_+ and N_- are the yields of a given state for incoming protons with spin up and spin down, respectively. The Basel sign convention is followed.

The relative errors shown are generally purely statistical, unless peak separation or background subtraction was difficult, in which case the errors were increased appropriately. The use of a peak-stripping computer program allowed us to obtain results for several states which were not included in Ref. 8. The absolute error due to uncertainty in the calibration of the beam polarimeter is about $\pm 5\%$.

A. $L=2$ Transitions

1. *Even-Even Nuclei*

Asymmetries for $L=2$ transitions in Mg^{24}, Mg^{26}, and Si^{28} are shown in Fig. 1. No two curves are precisely the same, and some of the variations are quite large. All, however, have two large peaks of positive asymmetry, with the possible exception of the 4.23-MeV

[6] See C. Glashausser and J. Thirion, in *Advances in Nuclear Physics*, edited by M. Baranger and E. Vogt (Plenum Press, Inc., New York, 1968), Vol. II, p. 79.

[7] H. Sherif and J. Blair, Phys. Letters **26B**, 489 (1968); H. Sherif, thesis, University of Washington, 1968 (unpublished); Nucl. Phys. **A131**, 532 (1969).

[8] A. Blair, P. A. Vaganov, C. Glashausser, J. Goudergues, R. M. Lombard, B. Mayer, R. de Swiniarski, and J. Thirion, Akad. Nauk SSSR Izv., Ser. Fiz. **32**, 814 (1968); [English transl.: Columbia Tech. Transl. **32**, 750 (1969)].

[9] G. M. Crawley and G. T. Garvey, Phys. Rev. **160**, 981 (1967).

[10] R. Beurtey and J. M. Durand, Nucl. Instr. Methods **57**, 313 (1967).

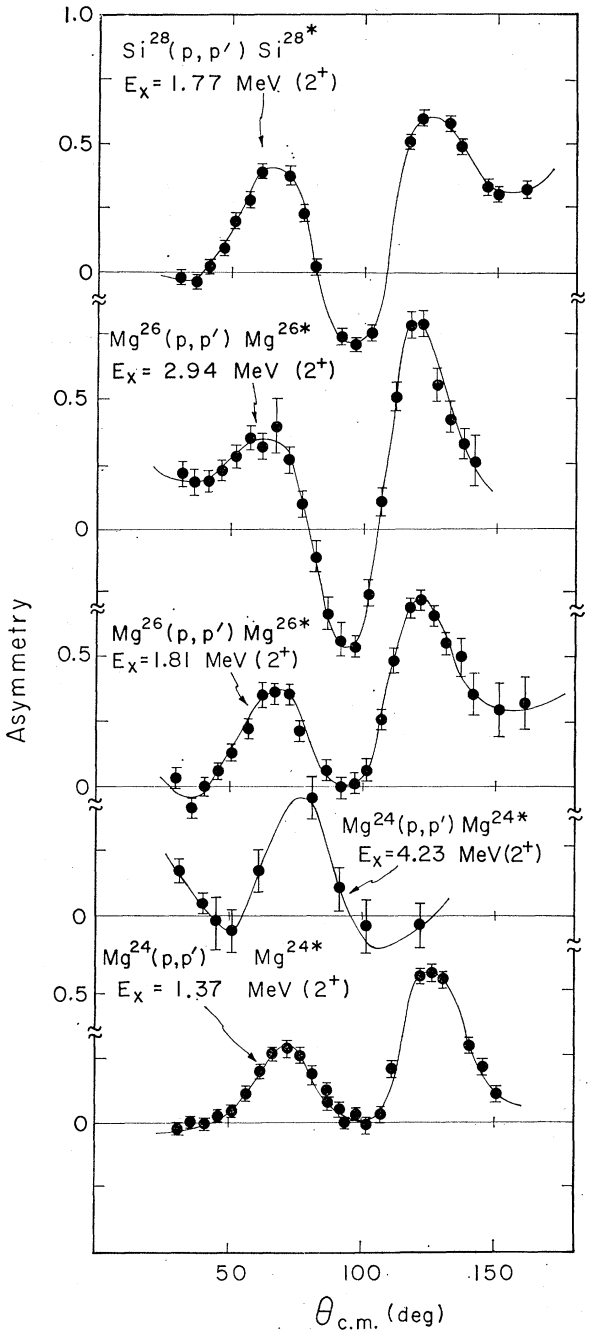

FIG. 1. Measured values of the asymmetry normalized to 100% beam polarization for $L=2$ transitions in Mg^{24}, Mg^{26}, and Si^{28}. The curves are visual guides.

state in Mg^{24}. The data for the first 2^+ (2^+_1) states in Mg^{24} and Mg^{26} are quite similar, but they are easily distinguishable from the Si^{28} data by the large dip in the latter curve around 100°. The asymmetry for the second 2^+ (2^+_2) state in Mg^{26} at 2.94 MeV shows larger oscillations than any of the other curves. The results for the 2^+_2 state in Mg^{24} are scanty but even these show differences from the other data.

Considerable variations are also observed in the differential cross sections at this energy, as well as at 17.5,[9] 49.5,[11] and 55 MeV.[12] At 49.5 MeV, e.g., the relative cross sections for the two 2^+ states in Mg^{24} are quite different. At 55 MeV, the shape and yield of the 2^+_1 states in Mg^{26} and Si^{28} are almost identical, but they are different from the results for the Mg^{24} 2^+_1 state. The cross section for the 2^+_2 state in Mg^{26} at 55 MeV deviates quite markedly from all these shapes. At the lower energies, 17.5 and 20.3 MeV, the cross section for the 2^+_1 state in Mg^{26} resembles that for the Mg^{24} 2^+_1 state more closely than that for the Si^{28} 2^+_1 state. The angular distributions of the 4^+_1 states in Mg^{24} and Si^{28} are also very different. The 20.3-MeV data are generally consistent with the 17.5-MeV data, but there are some differences in details, particularly at large angles. For example, the angular distributions for the two 2^+ states in Mg^{26} are very similar to each other at

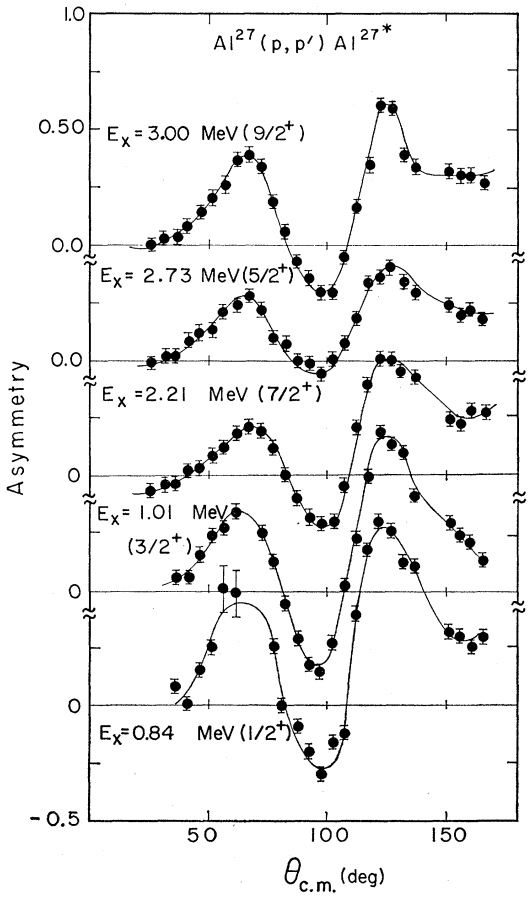

FIG. 2. Measured asymmetries for transitions in Al^{27}. The curves are visual guides.

[11] A. A. Rush and N. K. Ganguly, Nucl. Phys. **A117**, 101 (1968).

[12] J. Kokame, I. Nonaka, M. Koike, K. Matsuda, H. Kamitsubo, Y. Awaya, T. Wada, and H. Nakamura, in Proceedings of the International Conference on Nuclear Structure, Tokyo, 1967, p. 351 (unpublished).

20.3 MeV, while at 17.5 MeV a rather large difference between the two appears around 120°.

Since the structure of the nuclei is changing rapidly in this region of the Periodic Table, it is probably not surprising to find the variations observed in passing from one nucleus to the next. While Mg^{24} has a well-established rotational structure, the rotational structure of Mg^{26} is not apparent. Hartree-Fock calculations[13] of the ground state of Si^{28} indicate that a spherical solution lies considerably higher in energy than a deformed solution, but the oblate and prolate solutions lie close together. At the time the present experiments and calculations were performed, the deformed nature of Si^{28} had not yet received extensive confirmation. Very recently, however, Alexander *et al.* measured[14] the quadropole moment of the 2^+_1 state and determined that its shape is oblate. Bar-Touv and Goswami[15] have also indicated that the rotational model can explain the energy levels and transition rates in the ground-state

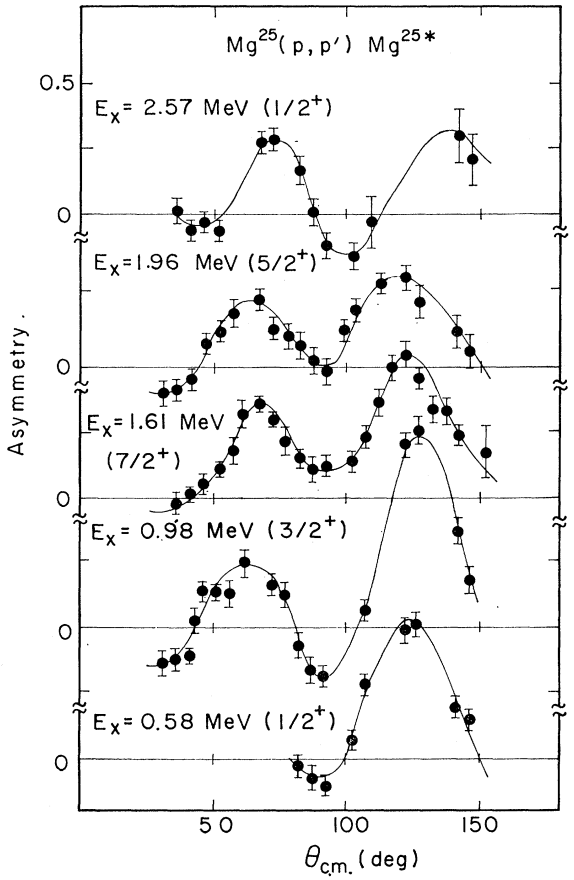

FIG. 3. Measured asymmetries for transitions in Mg^{25}. The curves are visual guides.

[13] G. Ripka, in *Advances in Nuclear Physics*, edited by M. Baranger and E. Vogt (Plenum Press, Inc., New York, 1968), Vol. I.

[14] T. K. Alexander, D. Pelte, O. Häusser, B. Hooton, and H. C. Evans, Bull. Am. Phys. Soc. **14**, 555 (1969).

[15] J. Bar-Touv and A. Goswami, Phys. Letters **28B**, 391 (1969).

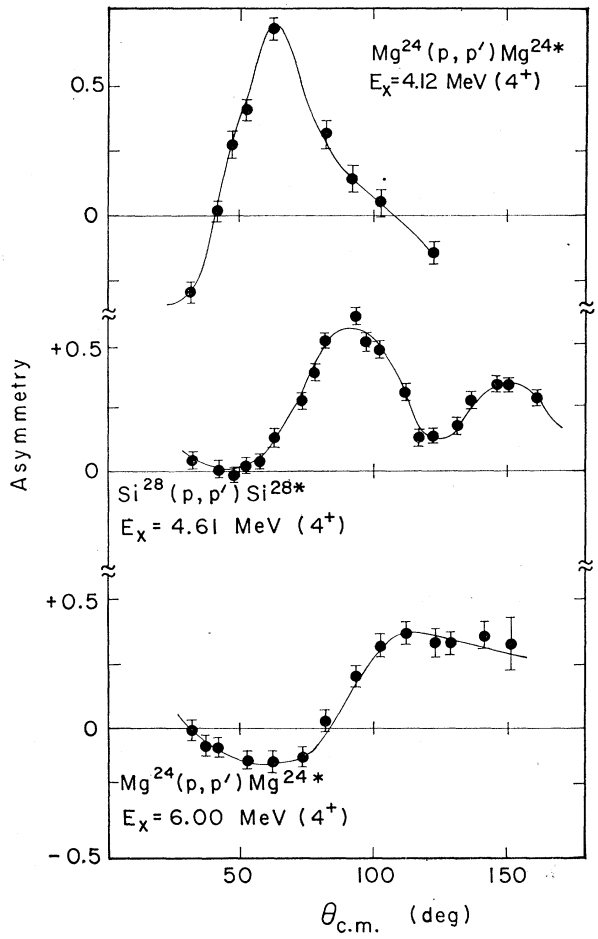

FIG. 4. Measured asymmetries for $L=4$ transitions in Mg^{24} and Si^{28}. The curves are visual guides.

band of Si^{28} very nicely provided some mixing with the spherical state is allowed. They assumed, however, that the 4.97-MeV level in Si^{28} is the spherical 0^+ state, and there is little experimental evidence to justify this assumption. Finally, differences in the 4^+_1 cross sections for Mg^{24} and Si^{28} at 17.5 MeV have been explained[16] as due to a large positive hexadecapole moment in the ground state of Si^{28}; Mg^{24} was found to have a very small, and possibly negative, hexadecapole moment.

2. Odd Nuclei

The weak-coupling model has been applied with considerable success to Al^{27}. This model provides a good explanation of the relative cross sections of the 0.842-($\frac{1}{2}^+$), 1.013-($\frac{3}{2}^+$), 2.212-($\frac{7}{2}^+$), 2.731-($\frac{5}{2}^+$), and 3.00-MeV ($\frac{9}{2}^+$) levels in Al^{27} and the 2^+_1 state in Si^{28} at 1.77 MeV, observed, e.g., in (p, p'),[9] (d, d'),[17] and

[16] R. de Swiniarski, C. Glashausser D. L. Hendrie, J. Sherman, A. D. Bacher, and E. A. McClatchie, Phys. Rev. Letters **23**, 317 (1969).

[17] H. Niewodniczański, J. Nurzyński, A. Stralkowski, J. Wilczynski, J. R. Rook, and P. E. Hodgson, Nucl. Phys. **55**, 386 (1964).

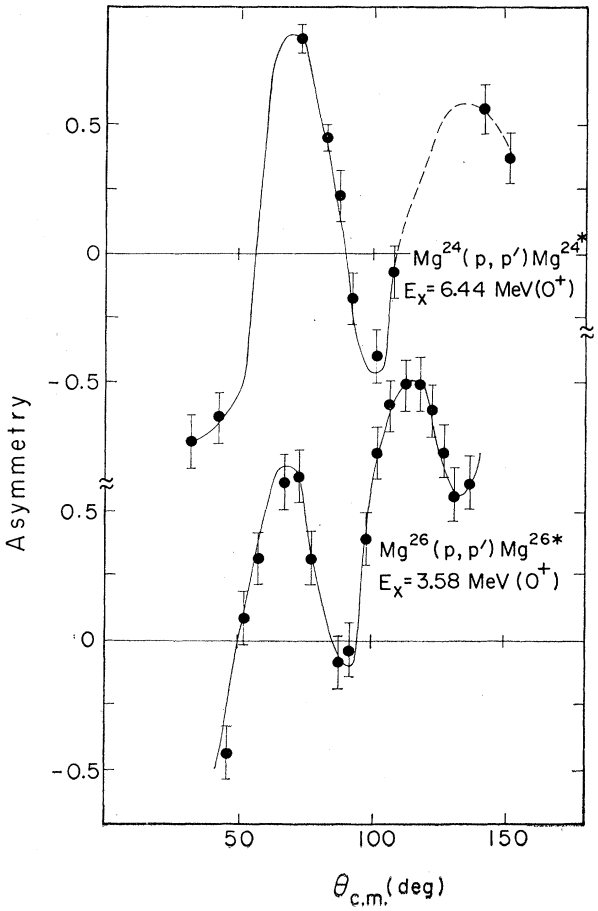

FIG. 5. Measured asymmetries for $L=0$ transitions in Mg^{24} and Mg^{26}. The curves are visual guides.

(e, e') [18] experiments. In its simplest form, all these Al^{27} levels except the $\frac{5}{2}^+$ states are supposed to arise simply from the coupling of a $d_{5/2}$ proton hole to the 2^+_1 state in Si^{28}. The $\frac{5}{2}^+$ ground state and the 2.731-MeV $\frac{5}{2}^+$ state are orthogonal combinations of a $d_{5/2}$ hole coupled to the 0^+ and the 2^+_1 state. The wave functions of these two $\frac{5}{2}^+$ states can then be written

$$\psi_{g.s.} = (1-A^2)^{1/2} \mid 0, \tfrac{5}{2}, \tfrac{5}{2}\rangle + A \mid 2, \tfrac{5}{2}, \tfrac{5}{2}\rangle,$$
$$\psi_{5/2^+}{}^* = -A \mid 0, \tfrac{5}{2}, \tfrac{5}{2}\rangle + (1-A^2)^{1/2} \mid 2, \tfrac{5}{2}, \tfrac{5}{2}\rangle. \quad (1)$$

The value of A has been determined[9] to be about 0.45.

With respect to the present data, the simple excited-core model predicts that the shapes of the differential asymmetries for the five excited states in Al^{27} should be the same as that for the 2^+_1 state in ^{28}Si. The data for Al^{27} are shown in Fig. 2. Note that the curves for the $\frac{1}{2}^+$, $\frac{3}{2}^+$, and $\frac{9}{2}^+$ states are very similar to each other and show the deep minimum at 100° characteristic of the 2^+_1 state of Si^{28}. However, the $\frac{5}{2}^+$ and $\frac{7}{2}^+$ curves show variations from the simple prediction. Both these states were cleanly resolved from neighboring states, whereas the $\frac{1}{2}^+$ and $\frac{3}{2}^+$ levels were separated with difficulty. The $\frac{9}{2}^+$ level at 3.00 MeV could not be separated from the $\frac{3}{2}^+$ level at 2.976 MeV, but there is evidence from the 17.5-MeV work[9] that the cross section is due almost entirely to excitation of the $\frac{9}{2}^+$ state. The deviations thus do not seem to be experimental in origin and should be ascribed to a failure of the simple model.

The model has not, in fact, been able to explain all previous data. The (p, p') cross sections for the states in Al^{27} show fair agreement in shape, but at both 17.5 and 20.3 MeV they show rather large deviations from the Si^{28} 2^+_1 distribution at angles larger than 80°. The differential cross section for the $\frac{7}{2}^+$ state in the Al^{27} (d, d') reaction[17] at 12 MeV was different from that of the other states; Bishop and Lombard[18] have observed that this state must retain some rotational character to explain their electron scattering results. However, if the discrepancy for the $\frac{7}{2}^+$ asymmetry can be ascribed to a rotational component in its wave function, it is not clear why this does not affect the $\frac{9}{2}^+$ distribution as well.

The strong-coupling model has generally been used to describe the levels of the other odd-A nucleus in

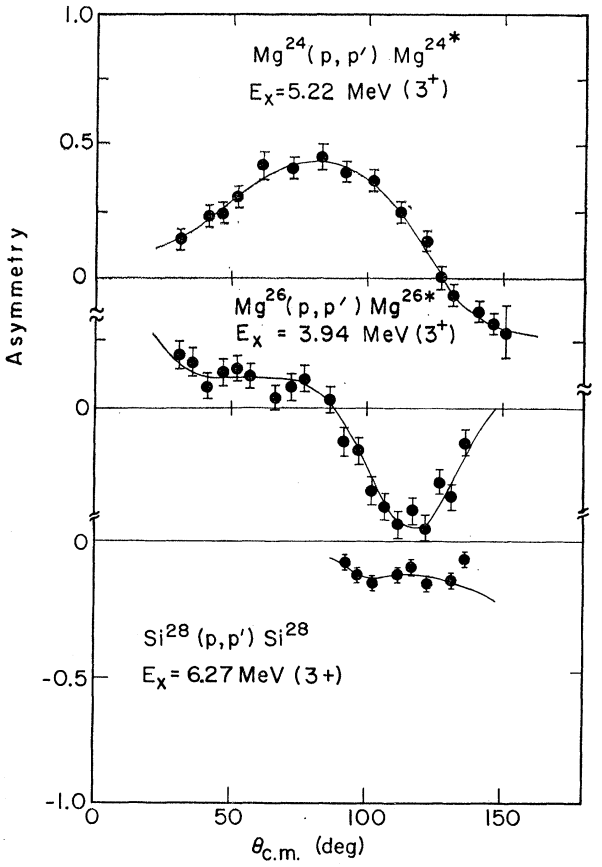

FIG. 6. Measured asymmetries for 3^+ states. The curves are visual guides.

[18] R. M. Lombard and G. R. Bishop, Nucl. Phys. **A101**, 601 (1967).

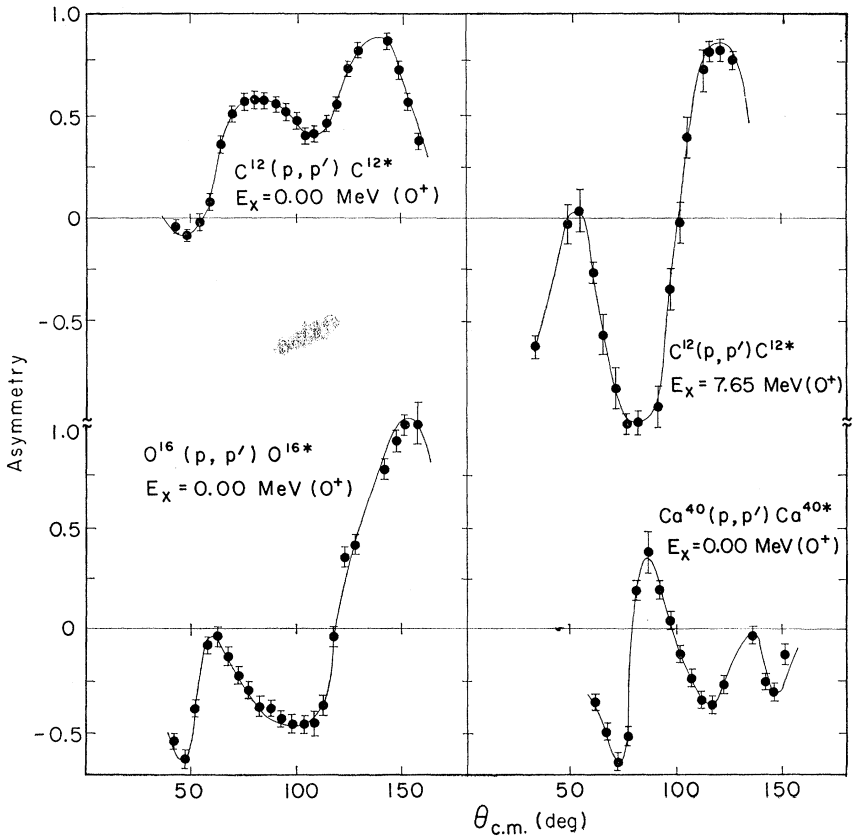

FIG. 7. Measured polarization in elastic scattering from C^{12}, O^{16}, and Ca^{40}. The asymmetry for the excited 0^+ state at 7.65 MeV in C^{12} is also shown. The curves are visual guides.

this investigation, Mg^{25}. Asymmetries measured for the low-lying states are shown in Fig. 3. The measured shapes of the differential cross sections at 17.5 MeV for all these states in Mg^{25} are very similar, and the same is true at this energy. The asymmetries, however, show large variations. The 1.61-MeV $\frac{7}{2}^+$ level is the second member of the rotational band built on the ground state; its cross section and asymmetry might thus be expected to closely resemble the corresponding curves for the 2^+_1 states in Mg^{24} or Mg^{26}. This prediction is certainly not precisely fulfilled, although the curves are more similar to the data for Mg^{24} or Mg^{26} than to the data for Si^{28}. The 0.58- ($\frac{1}{2}^+$), 0.98- ($\frac{3}{2}^+$), and 1.96-MeV ($\frac{5}{2}^+$) states are the low-lying members of a second rotational band built on a different particle state. The shapes of these asymmetry distributions are not necessarily expected to reflect the shapes of $L=2$ transitions in the neighboring nuclei or to exactly resemble each other. The variations observed are thus not unreasonable even in terms of the rotational model.

3. *L=4 Transitions*

Strong transitions to 4^+ states have been observed at 4.12 and 6.00 MeV in Mg^{24} and at 4.61 MeV in Si^{28}; the asymmetry data are illustrated in Fig. 4. Clearly, there is little similarity among the three curves. Differential cross sections for the two states in Mg^{24} are also very different from each other; the Si^{28} cross section is, however, similar in shape to the cross section for the 6.00-MeV state in Mg^{24}. As noted above,[16] the differences in the cross sections for the 4.12-MeV state in Mg^{24} and the 4.61-MeV state in Si^{28} can be explained if Si^{28} is assumed to have a large hexadecapole deformation.

4. *L=0 Transitions*

The asymmetries measured for the 0^+ states at 6.44 MeV in Mg^{24} and 3.58 MeV in Mg^{26} both show very large amplitude oscillations which are reminiscent of elastic scattering distributions. They are shown in Fig. 5. Cross sections for these states measured at 17.5 MeV were both strongly forward-peaked, but otherwise quite different from each other.

5. *Unnatural-Parity Transitions*

Transitions to 3^+ states were observed in the three even-even nuclei; the asymmetries are illustrated in Fig. 6. Clearly, there is no characteristic shape. The relative cross sections for all these states are rather flat at both 17.5 and 20.3 MeV; there is some structure but it is not the same at the two energies.

6. *C^{12}, O^{16}, and Ca^{40}*

The asymmetries for the ground states and for low-lying excited states in C^{12}, O^{16}, and Ca^{40} are shown in

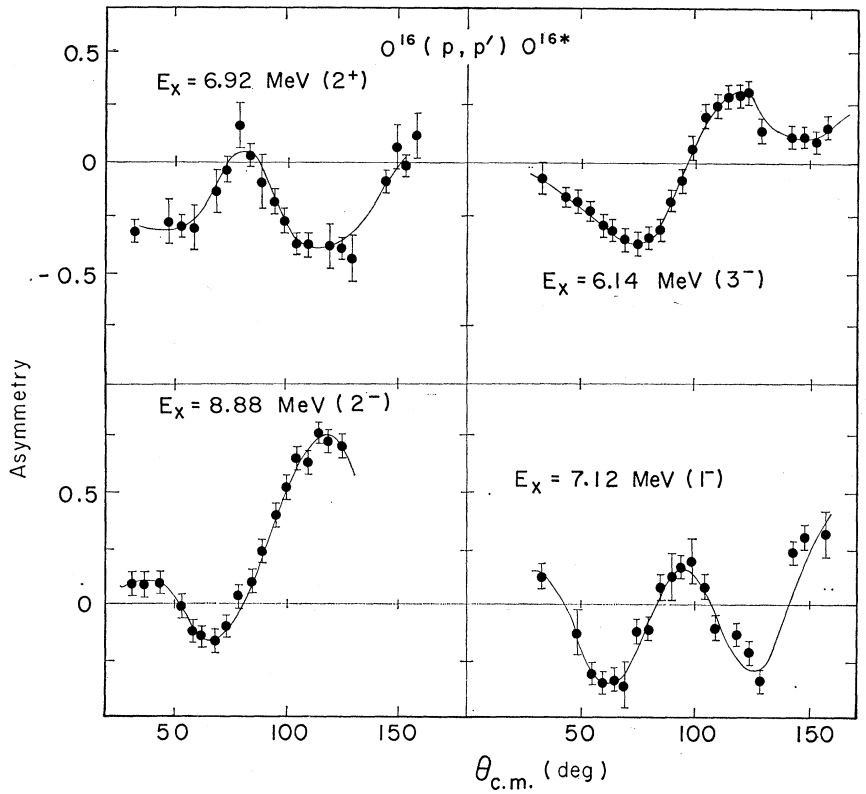

FIG. 8. Measured asymmetries for transitions in O^{16}. The curves are visual guides.

Figs. 7–9. The data for C^{12} are in only qualitative agreement with the data taken by Craig *et al.*[19] at 20.3 MeV; the discrepancies are probably due to the resonances observed at nearby energies. The present data were repeated many times over the course of several months with consistent results. In addition, the O^{16} data were taken at the same time. The elastic data for O^{16} agree well with the data of Boschitz *et al.*[20] at 20.7 MeV. However, Lowe[21] has reported resonance structure in O^{16} elastic scattering at 20.3 MeV; this makes the agreement between the 20.3- and the 20.7-MeV data surprising. The elastic data for Ca^{40} are in good agreement with data taken recently at Berkeley[22] at the same energy.

The curve in Fig. 7 showing the asymmetry for the excited 0^+ state in C^{12} at 7.65 MeV displays the same very large oscillations observed for 0^+ asymmetries in Mg^{24} and Mg^{26}. The asymmetries for the first 2^+ states in C^{12} and O^{16} at 4.43 and 6.92 MeV (Figs. 8–9) do not resemble each other or the curves for any $L=2$ transitions in Mg^{24}-Si^{28}. The data for the 3^- states in O^{16} and Ca^{40} are also quite different from each other. Note that the 3^- curve in Ca^{40} is completely out of phase with the 5^- curve. Finally, the asymmetries for the 1^- and 2^- states in O^{16} are also shown in Fig. 8.

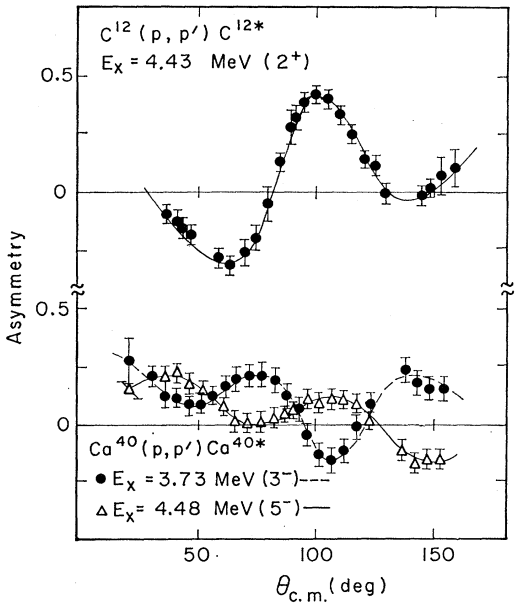

FIG. 9. Measured asymmetries for several transitions in C^{12} and Ca^{40}. The curves are visual guides.

[19] R. M. Craig, J. C. Dore, G. W. Greenlees, J. Lowe, and D. L. Watson, Nucl. Phys. **79**, 177 (1966).

[20] E. T. Boschitz, M. Chabre, H. E. Conzett, and R. J. Slobodrian, in *Proceedings of the Second International Symposium on Polarization Phenomena of Nucleons, Karlsruhe, 1965*, edited by P. Huber and H. Schopper (Birkhauser Verlag, Basel, 1966), p. 331.

[21] J. Lowe (private communication).

[22] R. de Swiniarski, A. D. Bacher, J. Ernst, A. Luccio, F. Resmini, R. Slobodrian, and W. Tivol, Bull. Am. Phys. Soc. **13**, 1663 (1968).

TABLE II. Optical-model parameters.

	V (MeV)	W_D (MeV)	V_{so} (MeV)	r_0 (F)	a_0 (F)	r_I (F)	a_I (F)	r_{so} (F)	a_{so} (F)	χ_σ^2	χ_p^2	χ^2/N	σ_R (mb)
Mg^{24}	47.8	8.46	5.15	1.21	0.61	1.14	0.54	0.97	0.32	37	301	8.68	711
Mg^{25}	42.82	6.88	4.18	1.26	0.67	1.42	0.37	1.04	0.34	80	178	6.32	665
Mg^{26}	55.43	9.68	9.00	1.15	0.67	1.31	0.42	0.80	0.97	117	137	5.34	744
Al^{27}	51.34	10.08	7.14	1.17	0.67	1.37	0.34	0.90	0.80	112	172	6.93	712
Si^{28}	45.57	7.91	4.08	1.20	0.65	1.44	0.41	0.97	0.35	76	185	7.31	760

IV. ANALYSIS

A. Optical Parameters ($Mg^{24}-Si^{28}$)

The determination of optical parameters for Mg^{24}-Si^{28} is complicated by the strong coupling between the excited states and the ground state. In their analysis of inelastic α scattering in the rare-earth region, Hendrie *et al.*[23] obtained excellent results by first obtaining optical-model parameters for a nearby spherical nucleus, and then using these same parameters in coupled-channel calculations for the deformed nuclei. Unfortunately, there is no nearby spherical nucleus to use as a starting point for the present analysis. In addition, it is not clear that the "spherical" parameters should remain constant, since the mass of these nuclei is low. The addition of spin also makes the parameter search more difficult. Finally, since we neglect possible spin-spin forces in the optical potential and the angular-dependent terms in the full Thomas form of the spin-orbit term in the optical potential, the parameters for odd-A nuclei might be expected to be somewhat different from the parameters for even-A nuclei.

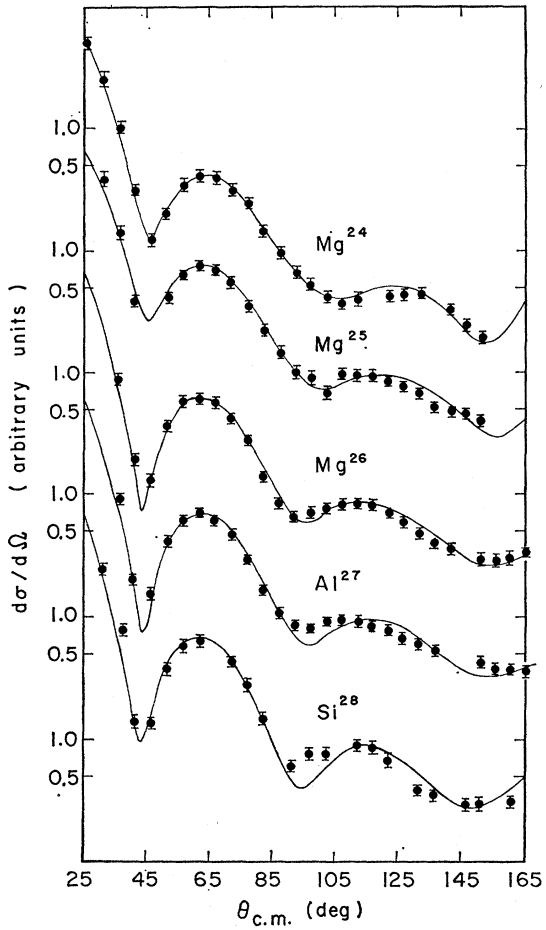

FIG. 10. Optical-model predictions of the elastic scattering cross sections. The parameters are those of Table II; no coupling was included.

The search code MERCY, a modified version of SEEK,[24] was used to obtain simultaneous fits to the elastic cross sections and polarizations; the coupling to the excited states was neglected. The definition of the optical potential and the search procedures employed are standard[1]; the absolute normalization of the data was included in the search. Errors on the cross sections were uniformly set at $\pm 10\%$; the errors on the polarization were fixed at ± 0.03. Corrections arising from the finite angular acceptance of the detectors were not included.

Calculations were carried out with three different sets of fixed geometrical parameters which have appeared in the literature.[25] The strength parameters V, W_D, and V_{so}, and the spin-orbit radius r_{so} were left as free parameters in the searches. The values of χ^2/N ranged from 9.0 for Mg^{25} to 28.5 for Si^{28}.

Since the fixed geometry searches did not yield very good fits to the data, a search on all nine parameters of the optical potential was performed. This search produced the fits to the elastic polarizations and cross sections shown in Figs. 10 and 11. These fits are still only fair, especially in comparison with the fits found in Ref. 1 for Zr^{90}, Zr^{92}, and Mo^{92}. The final parameter values are listed in Table II. The nucleus-to-nucleus variations are considerable, much larger than the variations in the parameters for the heavy nuclei. Some of these variations could be considerably reduced with little sacrifice in the quality of the fit. It is interesting

[23] D. L. Hendrie, N. K. Glendenning, B. G. Harvey, O. N. Jarvis, H. H. Duhm, J. Saudinos, and J. Mahoney, Phys. Letters **26B**, 127 (1968).

[24] M. A. Melkanoff, J. Raynal, and T. Sawada, University of California at Los Angeles Report No. 66-10, 1966 (unpublished).

[25] G. R. Satchler, Nucl. Phys. **A92**, 273 (1967); F. G. Perey, Phys. Rev. **131**, 745 (1963); P. Kossanyi-Demay and R. de Swiniarski, Nucl. Phys. **A108**, 577 (1968).

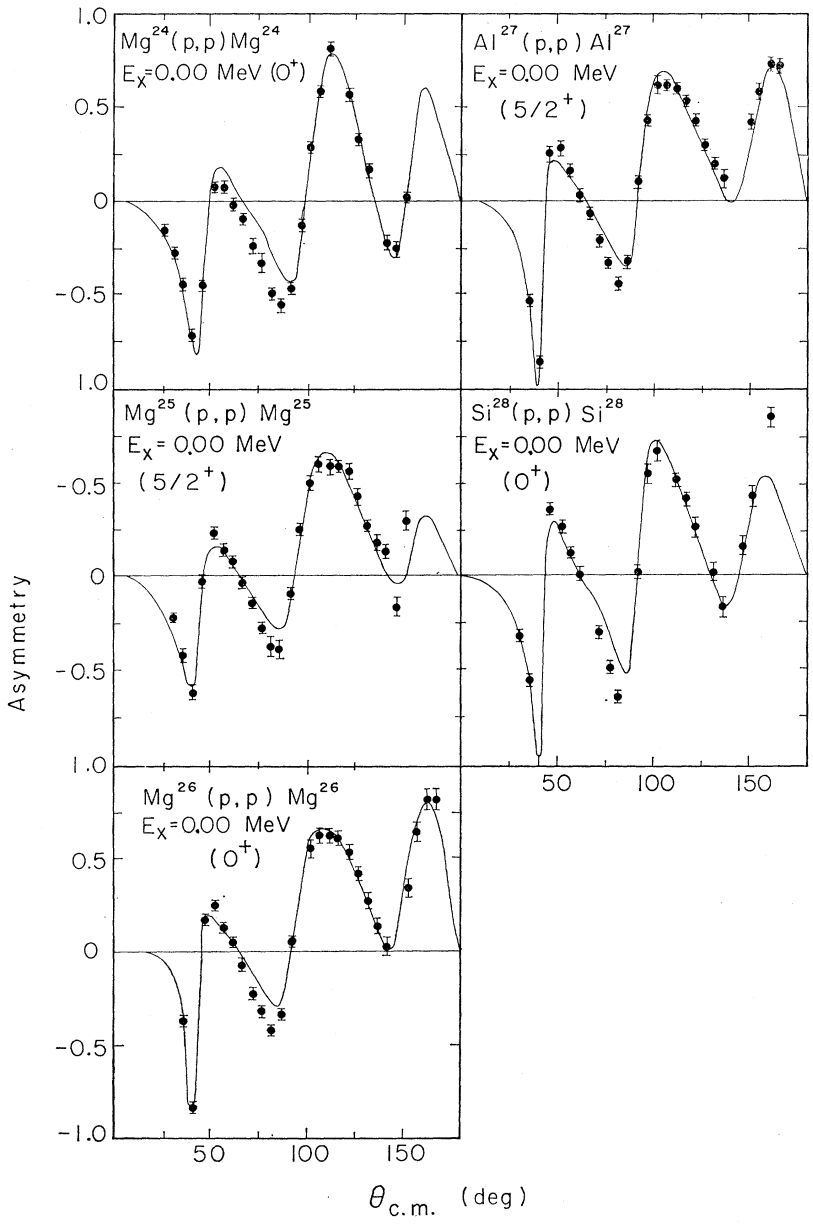

FIG. 11. Optical-model predictions of elastic scattering polarization. The parameters are those of Table II; no coupling was included.

to note that r_{so} is generally at least 20% smaller than the central radius; in heavier nuclei this difference is usually about 10–15%.

Since it has sometimes been found necessary[4] to have very good fits to the elastic polarization in order to obtain good fits to inelastic asymmetry data, searches were also made on the polarization data alone for Mg^{24} and Si^{28}. However, the best fits are very little better than those illustrated in Fig. 11. Better fits were obtained by including an imaginary spin-orbit term with a strength between 0.0 and +1.0 MeV. However, the inclusion of this term makes the 2^+ asymmetry predictions considerably worse.

B. Coupled Channels and DWBA

The Oxford coupled-channel program[26] was used to interpret the inelastic scattering cross sections and asymmetries. Both rotational and vibrational models are allowed; the entire optical potential can be deformed. In the vibrational model, terms up to second order in the Taylor expansion of the optical potential can be included. In the rotational model, on the other hand, the calculation is correct to all orders in the interaction potential, since a Legendre expansion is used. In the small coupling limit, where the DWBA

[26] A. D. Hill (unpublished).

is valid, the two models give the same results. When the coupling is sufficiently strong, however, the predictions need not be similar, and cross-section and asymmetry measurements can, in principle, distinguish between the models. However, the predictions for the vibrational model may be sensitive to the number of terms retained in the Taylor expansion.

Both the vibrational and rotational models assume that the nuclear surface should be represented by the shape

$$R(\theta, \phi) = R_0[1+\Phi(\theta, \phi)],$$

where

$$\Phi(\theta, \phi) = \sum_{\lambda\mu} \alpha_{\lambda\mu} Y_\lambda^\mu(\theta, \phi);$$

$\alpha_{\lambda\mu}$ is directly related to the deformation parameter β_λ and $Y_{\lambda\mu}$ is a spherical harmonic. In the rotational model, β represents the static deformation of the nucleus in the rotational band built upon the ground state. In the vibrational model, β is a dynamical deformation parameter which describes the amplitude of the vibrations about a spherical equilibrium state. The form that the optical potential $U(r)$ takes under this deformation is not well defined.[6] Two methods have generally been used. The first is to replace $U(r)$ by $U(r-R)$. The second is to replace R_0, whenever it appears in the undeformed potential, by $R(\theta)$. The two methods give equivalent descriptions of the inelastic scattering provided the deformation of the spin-orbit term in the potential is not important. The two methods do not, however, yield equivalent forms of the deformed-spin-orbit term (DSO). The first method yields the form used in previous vibrational-model calculations by the Saclay group.[1] It will be referred to as type I:

$$V_{so}(r) = (R_0/a^2r^2)\,2e(1+e)^{-3}[a(1+e)+r(e-1)], \quad (2)$$

where e is $\exp[r-R_0A^{1/3}/a]$. The second method has been used by the Oak Ridge group[4] and others, and yields the form which will be referred to as type II:

$$V_{so}(r) = (R_0/a^2r^2)\,2e(1+e)^{-3}[r(e-1)]. \quad (3)$$

Note that type I includes an extra term inside the brackets.

In addition to these two methods, the full Thomas (FT) form of the DSO potential has also been used with success by Sherif and Blair.[7] They write the spin-orbit term in the optical potential as follows:

$$U_s(r, \theta, \phi) = (\hbar/m_\pi c)^2\sigma\cdot[\nabla\rho(\mathbf{r})\times\nabla/i], \quad (4)$$

where $\rho(\mathbf{r})$ is the nuclear matter density. If the angular dependence of the gradient operator acting on $\rho(\mathbf{r})$ is neglected, this expression reduces to the standard $\mathbf{l}\cdot\boldsymbol{\sigma}$ form. The angle-dependent terms can affect the inelastic predictions, and generally they have been found[7] to improve the fits to inelastic asymmetry and spin-flip data. The Oxford program does not include the FT form, but some DWBA calculations have been carried out with the program of Sherif and the results are described below. The radial part of the FT DSO potential in his program is equivalent to the type-II term above.

Coupled-channel calculations with type-I and type-II terms have been performed for the 0^+, 2^+_1, and 4^+_1 states in Mg^{24} and Si^{28}. Our primary interest, of course, lies in the quality of the predictions of the 2^+_1 and 4^+_1 asymmetries. However, we also want to know whether the asymmetry data can distinguish between

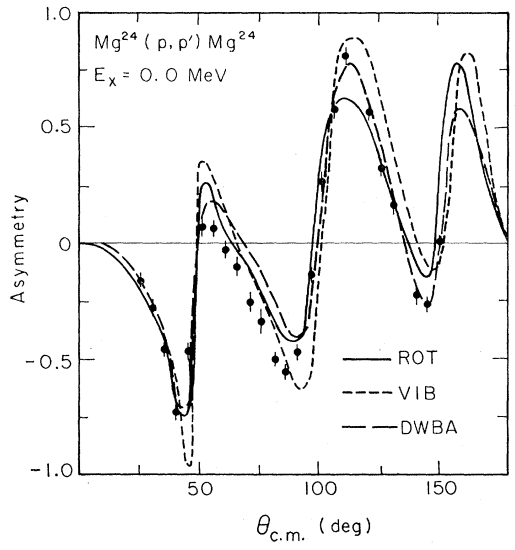

FIG. 12. Coupled-channels calculations of the elastic scattering polarization. The rotational and first-order vibrational model curves assume a β_2 of 0.49. The curve labeled DWBA was calculated with a β_2 of 0.01 with the coupled-channels program.

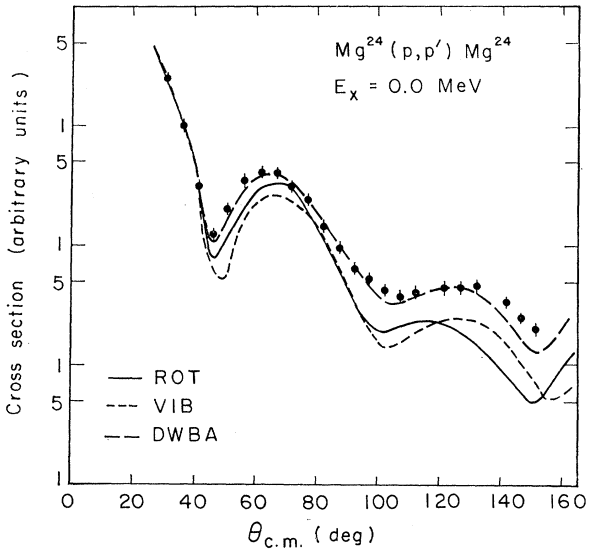

FIG. 13. Coupled-channel calculations of the elastic scattering cross sections. The deformation parameters are the same as for Fig. 12.

rotational and vibrational models, and between positive and negative deformations. The CC calculations shown here used optical parameters which were not adjusted from the spherical values; only the fine details of the asymmetry predictions are affected when the adjusted values are used.

1. Elastic Scattering and Polarization

When the parameters of Table II are used in a CC calculation, the predicted elastic scattering polarization and cross section are changed considerably. This comparison is illustrated in Figs. 12 and 13 for Mg^{24}. A deformation parameter β_2 of 0.49 was assumed for the rotational- and vibrational-model calculations and coupling to the first 2^+ and 4^+ states was included. The curves labeled DWBA are the spherical optical-model fits to the data; they are identical to those shown in Figs. 10 and 11. The quality of the fit to the elastic polarization data between 60° and 90° is improved when the strong coupling is included; at back angles, however, the CC fit is somewhat worse. For the cross section, the DWBA fit is considerably better than the other two.

If the spherical optical-model parameters are adjusted by decreasing V_0 and W_D, the CC fit to the cross section can be made almost as good as the spherical fit. When this is done, the CC polarization prediction is almost identical to the spherical prediction at angles up to 100°. To improve the CC polarization fit at back angles requires finer parameter adjustments.

Further calculations show that the predictions of both the elastic polarization and the cross section are little affected by the inclusion of the 4^+_1 state unless some β_4 deformation is added. The predictions do depend, of course, on whether the entire optical potential is deformed, or just certain parts of it. For the curves of Figs. 12 and 13, all terms, real, imaginary, and spin-orbit, were deformed. The predictions of the elastic scattering are not sensitive to the type of spin-orbit deformation.

2. 2^+ States

Predictions of the asymmetry and cross sections for the 2^+_1 state in Mg^{24} and Si^{28} are shown in Figs. 14 and 15. All curves illustrated have been calculated with the entire optical potential deformed, since the predictions of the asymmetry are almost invariably improved by the inclusion of deformed imaginary and spin-orbit terms. The DSO term has little effect on the cross sections; the effect of complex coupling on the cross-section predictions is variable. In the CC calculations shown, the ground state, the 2^+_1 state, and the 4^+_1 state have generally been included. When no direct transition to the 4^+_1 state was allowed, i.e., when β_4 was set to zero, the 4^+_1 state could be omitted from the CC calculation with almost no effect on the 0^+ and 2^+ predictions.

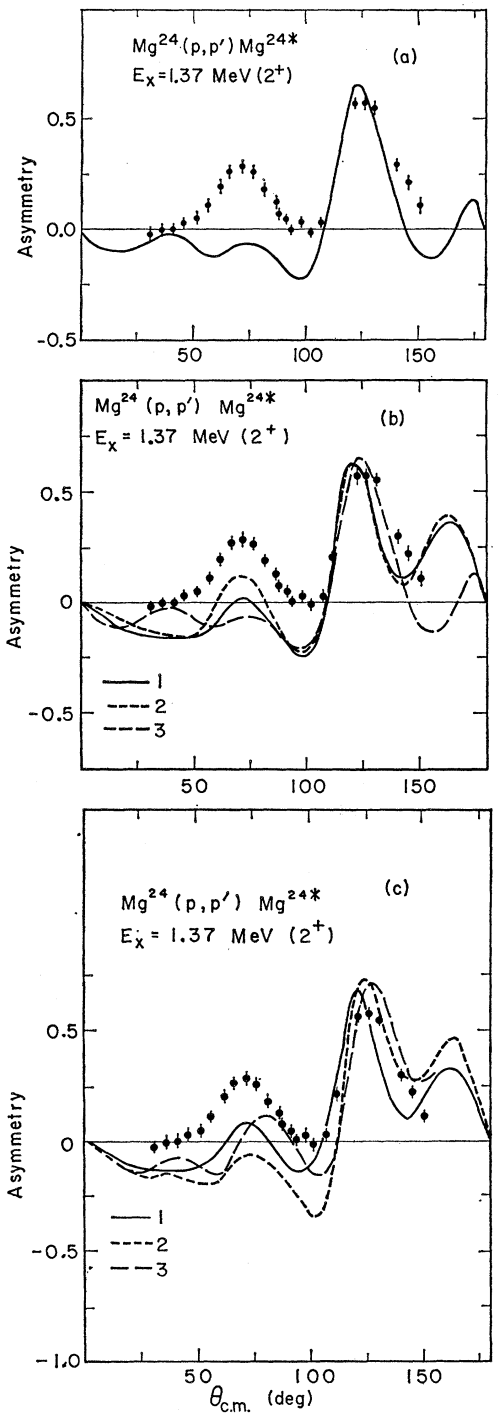

FIG. 14. Predictions of the asymmetry for the 1.37-MeV 2^+ state in Mg^{24}. (a) CC rotational-model prediction, type-II DSO, $\beta_2=0.49$. (b) (1) DWBA prediction, type-II DSO. (2) DWBA prediction, FT spin-orbit term. (3) CC rotational-model prediction, type-II DSO, $\beta_2=0.49$. (c) (1) DWBA prediction, type-I DSO. (2) CC vibrational-model prediction, first-order, type-I DSO, $\beta_2=0.49$. (3) CC vibrational-model prediction, second-order, type-I DSO, $\beta_2=0.49$.

The value of β_2 for Mg^{24} was set to +0.49, the value obtained in a CC analysis of 49.5-MeV inelastic proton scattering by Rush and Ganguly.[11] Since absolute cross sections were not obtained in the present work, this value could not be checked. However, a very similar value +0.47 has been recently obtained from the CC analysis of 17.5-MeV proton scattering.[16] For Si^{28}, the value of β_2 was generally set at 0.55, the value obtained in several DWBA analyses of proton scattering.[9,27] However, the CC analysis of the 17.5-MeV data[16] gives a β_2 of about 0.34. Thus, the effects of the strong coupling are somewhat overestimated for Si^{28}. When a nonzero value of β_4 was included in the present calculations, it was set to +0.33. The values of β_4 obtained from the 17.5-MeV analysis[16] are −0.05 for Mg^{24} and +0.25 for Si^{28}.

The CC rotational-model prediction for the 2^+_1 asymmetry in Mg^{24} is shown in Fig. 14(a); a type-II DSO term was used with the optical parameters of Table II. It is clear that the forward maximum is not predicted, whereas the back-angle peak is fitted fairly well. If the parameters are adjusted to fit the elastic cross section, almost no change is observed in the predicted asymmetry of the 2^+_1 state. The forward maximum appears also in data at higher energies,[4,11] at smaller angles; the high-energy fits are also poor at this maximum, unless the magnitude of the DSO term is arbitrarily increased.

Curves 1 and 2 in Fig. 14(b) correspond to DWBA calculations with a type-II DSO term, with and without the angle-dependent term of the FT spin-orbit potential. The CC rotational-model calculation (curve 3) is the curve of Fig. 14(a). Note that the effect of including

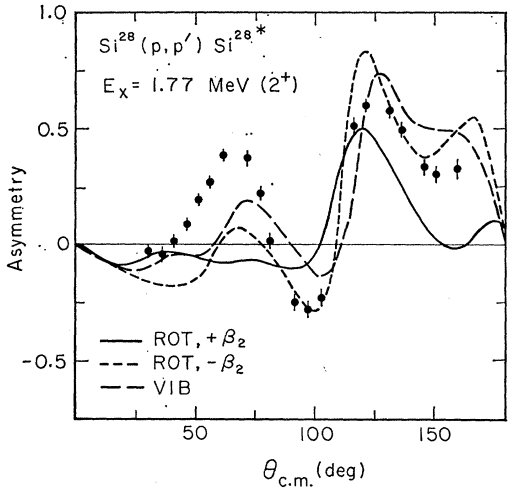

FIG. 15. Predictions of the asymmetry for the 1.77-MeV 2^+ state in Si^{28}. (1) CC rotational-model prediction, type-II DSO, $\beta_2=0.55$. (2) Same as (1) but $\beta_2=-0.55$. (3) CC vibrational-model predictions, second-order, type-I DSO, $\beta_2=0.55$, $\beta_4=0.33$.

[27] R. W. Barnard and G. D. Jones, Nucl. Phys. **A108**, 655 (1968).

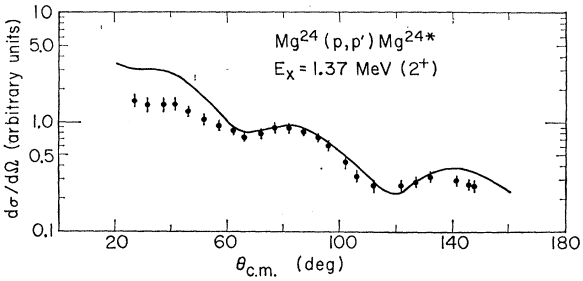

FIG. 16. Predicted cross section for the 2_1^+ state of Mg^{24}; the CC rotational-model was used with $\beta_2=0.49$.

the strong coupling in the calculation is to reduce the predicted maximum near 70°, while including the FT term increases it (curve 2).

Illustrated in Fig. 14(c) are three curves with a type-I DSO term. The DWBA prediction (curve 1) is positive at the 70° maximum, and is quite similar to the FT curve (2) in Fig. 14(b). The radial part of the FT DSO term is of type II. The fact that curve 1 is similar to the FT prediction indicates that the FT prediction could be improved by including a type-I radial part instead of type II. The other two curves in Fig. 14(b) are CC vibrational-model calculations with the expansion extended to first and second order, respectively. Including the first-order coupling (curve 2) decreases the 70° maximum considerably; the second-order term increases it again, but shifts it out of phase (curve 3). Since the difference between curves 2 and 3 is so large, it is reasonable to assume that some of the differences between the rotational-model calculations [Fig. 14(a)] and these vibrational-model calculations may be due to the neglect of third- and higher-order terms in the vibrational expansion.

Some CC predictions for Si^{28} asymmetries are shown in Fig. 15. The three curves correspond to rotational-model calculations (type II) with $\beta_2=+0.55$ (1), and $\beta_2=-0.55$ (2), and a second-order vibrational-model calculation (type I) with $\beta_2=0.55$ and $\beta_4=0.33$. Since the recent measurement of the quadrupole moment of the 2^+_1 state indicates that Si^{28} has an oblate deformation,[14] we should expect the rotational-model prediction with a negative β_2 to give the best agreement. In fact, the oblate prediction is better than the prolate prediction, but both are far from reproducing the forward maximum. It is interesting, however, that the measured asymmetry for Si^{28} at the 70° maximum is more positive than for Mg^{24}; at least this difference is predicted by the calculations. However, both rotational-model predictions are worse than the vibrational-model curve, although the neglect of third- and higher-order terms may be important, as discussed above. Note finally that for a given type of calculation the asymmetry predictions for Mg^{24} and Si^{28} are very similar, even though the optical parameters of Table II are quite different.

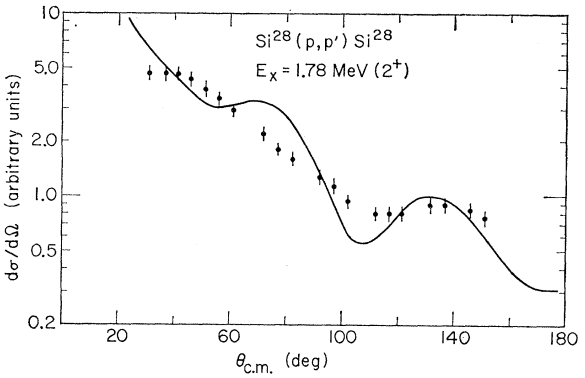

FIG. 17. Predicted cross section for the 2_1^+ state of Si^{28}; the CC rotational-model was used with $\beta_2=-0.55$, $\beta_4=0.33$.

The fits to the cross sections shown in Figs. 16 and 17 are fair. Rotational-model CC curves are shown, β_2 is positive for Mg^{24} and negative for Si^{28}. The parameters of Table II are used. The main effect of adjusting these parameters to fit the elastic scattering is to change the absolute magnitude of the predictions, but the normalization here is arbitrary. However, the modifications also tend to improve the fits at back angles. Many other cross-section predictions have been made, with different values of β, with different optical parameters, and with the vibrational model. Generally, the differences between these predicted angular distributions are too small to be experimentally distinguishable.

3. 4^+ States

The 4^+ state of a rotational band built upon a 0^+ ground state cannot be excited in first order unless the nucleus has a hexadecapole deformation. A two-phonon state in a vibrational model must also be excited by a multiple-excitation process, whereas a one-phonon vibrational state can be excited in first order. Predictions of the asymmetry for the 4^+_1 states in Mg^{24} and Si^{28} for these modes of excitation are shown in Figs. 18 and 19. Type-I DSO terms were used in the vibrational-model calculations, and type-II DSO terms were used in the rotational-model calculations. Agreement with the experimental data is uniformly poor.

Illustrated in Fig. 18(a) is the CC rotational-model curve for Mg^{24} with β_2 only (β_4 was found to be very small in the work of Ref. 16). Again, the prediction is not sensitive to the optical parameters.

The predictions of other model assumptions are shown in Fig. 18(b). Curve (1) is the same type of calculation as shown in Fig. 18(a), but β_4 deformation has been included. Curve (2) is a CC vibrational-model calculation for a two-phonon 4^+ state, with β_2 only. Curve (3) is a CC vibrational-model calculation for a one-phonon 4^+ state; both β_2 and β_4 are included. The differences between the predicted curves are quite large, but none gives any hint of a large peak at about 60°. The two-phonon prediction (curve 2) is reasonably similar to the curve of Fig. 18(a); neither includes first-order contributions. The two curves (1 and 3) which do include first-order contributions are similar at forward angles.

The rotational-model prediction for Si^{28} is shown in Fig. 19(a); β_2 and β_4 are included. The inclusion of β_4 was necessary to account for the shape and magnitude of the 17.5-MeV cross section, but it does not improve the fit to the asymmetry. In Fig. 19(b) are two DWBA curves, the one with a type-I DSO term, and the other with the FT term. The two are very similar and fail to reproduce the data.

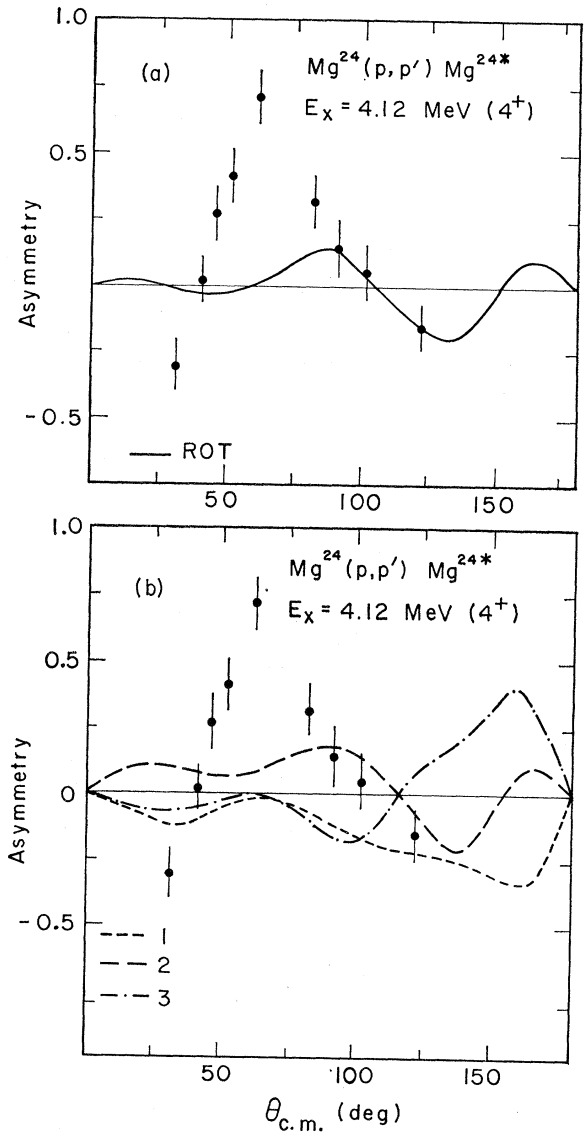

FIG. 18. Predicted asymmetries for the 4_1^+ state of Mg^{24}. (a) CC rotational-model prediction, type-II DSO, $\beta_2=0.49$. (b) (1) CC rotational-model prediction, type-II DSO, $\beta_2=0.49$. $\beta_4=0.30$. (2) CC vibrational-model calculation, type-I DSO, one-phonon state, $\beta_2=0.49$, $\beta_4=0.30$. (3) CC vibrational-model calculation, type-I DSO, two-phonon state, $\beta_2=0.49$.

The fits obtained to the 4^+_1 cross sections for Mg^{24} and Si^{28} are presented in Figs. 20 and 21. The CC rotational-model curve for Mg^{24} with β_2 only (Fig. 20) does not give a good fit with the parameters of Table II; readjusting the parameters to fit the elastic scattering improves the agreement at back angles. The CC rotational-model prediction for Si^{28} (Fig. 21) includes β_4 and gives a reasonably good fit to the data. Without β_4, the prediction is very similar to the prediction for Mg^{24}. Vibrational-model calculations for the 4^+ states

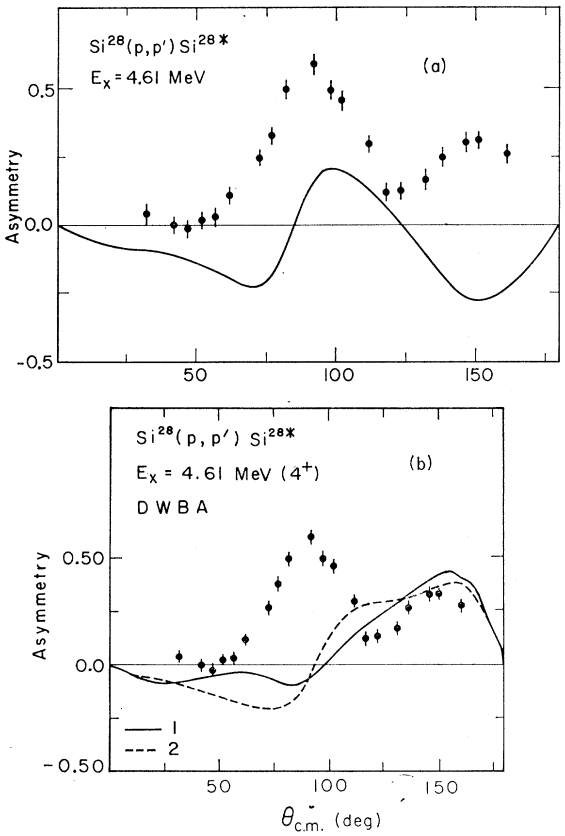

FIG. 19. Predicted asymmetries for the 4_1^+ state of Si^{28}. (a) CC rotational-model prediction, type-II DSO, $\beta_2=-0.55$, $\beta_4=0.33$. (b) (1) DWBA prediction, type-I DSO term. (2) DWBA prediction, FT spin-orbit term.

closely resemble the rotational-model calculations. The rotational-model curve calculated without β_4 resembles a two-phonon vibrational-model curve; with β_4, the rotational-model prediction is similar to a one-phonon vibrational-model prediction.

4. Ca^{40}

Both macroscopic and microscopic calculations have been carried out for the first 3^- and 5^- states in Ca^{40}. The microscopic curves have been calculated by Schaeffer[28]

[28] R. Schaefer (private communication).

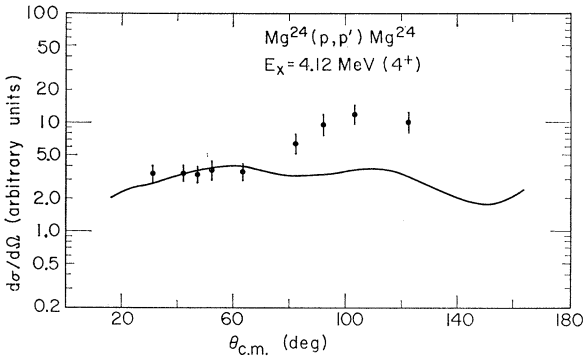

FIG. 20. Predicted cross section for the 4_1^+ state in Mg^{24}; the CC rotational model was used with $\beta_2=0.49$.

using the wave functions of Gillet and Sanderson.[29] The cross sections and asymmetries that he has computed are shown in Figs. 22 and 23. The contribution of the knock-on exchange amplitudes has been included to a good approximation in some of these curves; a Serber exchange mixture was assumed. The effects of exchange on the absolute magnitude of the predicted cross sections are large and clearly important; however, the shapes of the asymmetries and differential cross sections are not grossly changed. The asymmetry for the 5^-_1 state shows reasonable agreement, either with or without exchange, but the cross section does not; for the 3^-_1 state, the cross-section prediction is reasonably good, but the asymmetry is poorly fit.

The DWBA macroscopic-model predictions of the asymmetry are illustrated in Fig. 24. The fits are somewhat better than the fits obtained with the microscopic model. The full Thomas term improves the fit to the asymmetry of the 5^-_1 state but makes the agreement for the 3^-_1 state somewhat worse. The good agreement with the 5^-_1 state is interesting because it indicates that the difficulties with the 4^+_1 states in Mg^{24} and Si^{28}

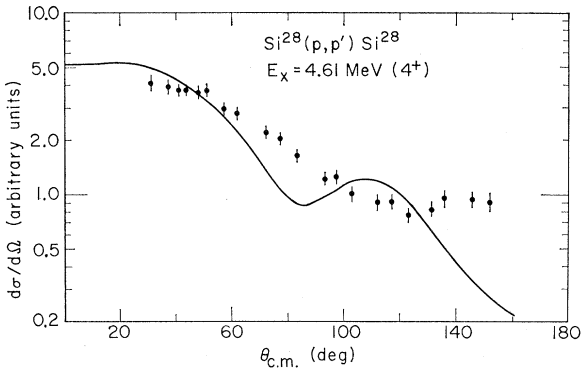

FIG. 21. Predicted cross section for the 4_1^+ state in Si^{28}; the CC rotational model was used with $\beta_2=-0.55$, $\beta_4=0.33$.

[29] V. Gillet, A. Green, and E. Sanderson, Nucl. Phys. **88**, 321 (1966); V. Gillet and E. Sanderson, *ibid.* **91**, 292 (1967).

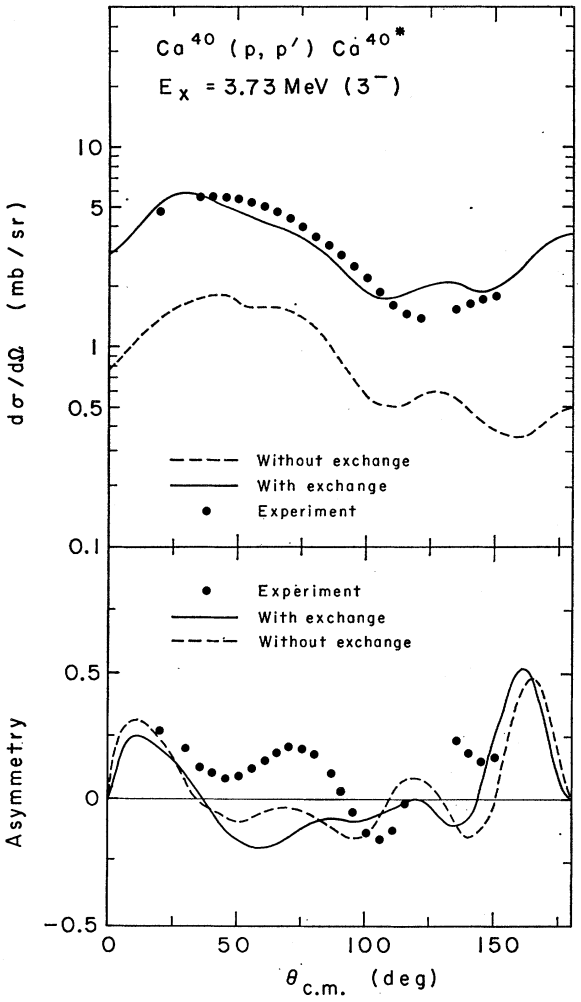

FIG. 22. Microscopic-model predictions of the asymmetry and cross section for the 3_1^- state in Ca^{40}, calculated by R. Schaeffer.

do not arise simply because of the high spin of these states.

V. SUMMARY AND DISCUSSION

Asymmetries measured for a given value of the angular momentum transfer show rather large differences from one nucleus to the neighboring one, although some gross features of the curves remain constant, such as the peaks at 70° and 120° for $L=2$ transitions. The differential cross sections for a given L transfer also vary widely. The shapes, however, generally agree quite well with those measured by Crawley and Garvey[9] at 17.5 MeV. In addition, the forward peak in the $L=2$ asymmetries has also been observed at 30, 40, and 49 MeV. These two observations indicate that compound-nucleus contributions are not important, except perhaps for excited 0^+ states and unnatural-parity states which have small cross sections. Some discrepancies with the predictions of a pure weak-coupling model for Al^{27} were found, especially in the shapes of the asymmetries for the $\frac{5}{2}^+$ and $\frac{7}{2}^+$ levels at 2.73 and 2.21 MeV. Very large asymmetries were measured for excited 0^+ states, comparable in magnitude to the polarization in elastic scattering. The shapes of the asymmetry curves for 3^+ states showed the largest nucleus-to-nucleus variations.

The theoretical analysis of the 2^+_1 and 4^+_1 asymmetries in Mg^{24} and Si^{28} yielded disappointing results. These results must be considered preliminary in the sense that no search was made on the optical parameters with the effects of strong coupling included. However, it is unlikely that a set of optical parameters can be found to reproduce the 2^+ and 4^+ asymmetries. We have, in fact, tried a large number of parameter sets without success; the predictions are not very sensitive to the parameters. Further, the one adjustment of the

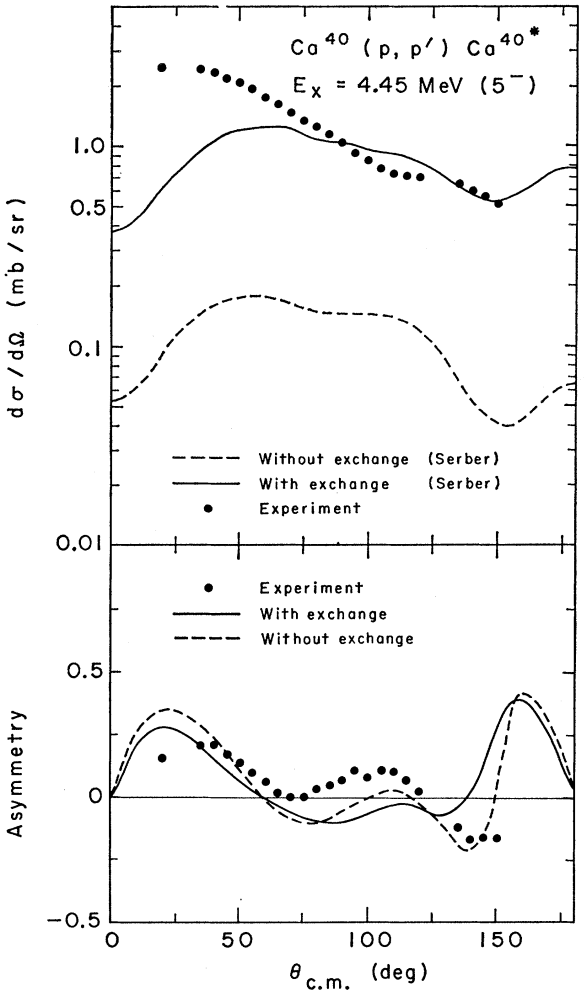

FIG. 23. Microscopic-model predictions of the asymmetry and cross section for the 5^- state in Ca^{40}, calculated by R. Schaeffer.

optical parameters which does make a significant improvement in the fits to the elastic polarization, viz., the inclusion of a positive imaginary spin-orbit potential, makes the fits to the asymmetries considerably worse.

The effects of strong coupling are important in describing both the elastic and inelastic asymmetries and cross sections. Differences were usually found between the predictions of the rotational and vibrational models, but neither gave a good fit to the data for $L=2$ or $L=4$ transitions. Some of the differences between the two models may be due to the neglect of terms of higher than second order in the vibrational-model expansion.

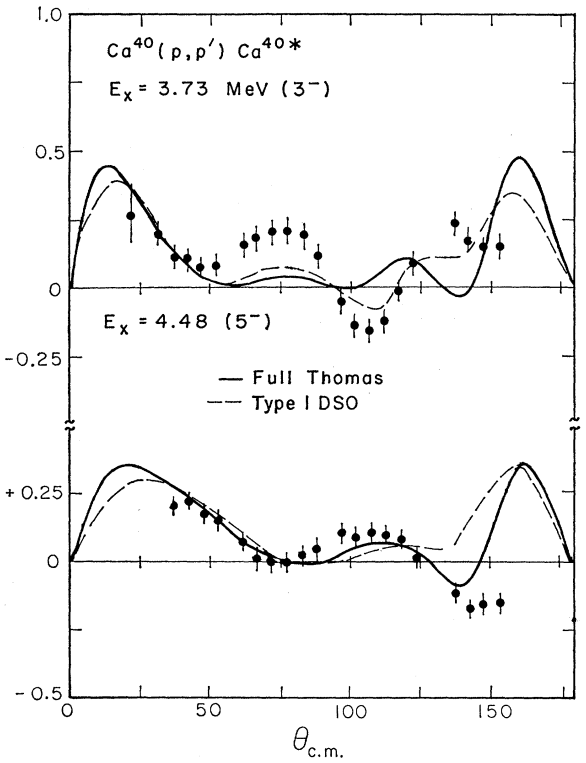

FIG. 24. DWBA predictions of the asymmetries for the 3_1^- and 5_1^- states in Ca^{40} with FT and type-I DSO terms.

The predicted asymmetries for Si^{28} with a positive and a negative deformation parameter are also significantly different, but both are in poor agreement with the data. The analysis of the 4^+_1 asymmetries in Mg^{24} and Si^{28} adds no new information on the hexadecapole deformations of these nuclei.

Calculations were performed with two different types of radial dependence in the deformed spin-orbit term, and also with the FT expression of the spin-orbit term. The type-I predictions [Eq. (2)] were consistently better than the type-II predictions [Eq. (3)] for $L=2$ transitions. Differences between these two types of calculation have previously been found to be very small for heavier nuclei. The FT predictions are also superior to the type-II curves; a comparison[30] of a rotational-model CC curve with an FT (DWBA) prediction reveals a clear preference for the latter. However, the FT (DWBA) and type-I (DWBA) predictions can hardly be distinguished from each other.

Microscopic- and macroscopic-model DWBA predictions of the asymmetries of the 3^-_1 and 5^-_1 states in Ca^{40} yielded fair agreement with the experimental data. The vibrational model fit to the 5^- asymmetry is quite good, in fact, when the FT term is included. Thus the failure to obtain good fits to the 4^+ states in Mg^{24} and Si^{28} cannot be ascribed simply to the high spin.

ACKNOWLEDGMENTS

The authors are grateful for the indispensable help of the technical staff at the Saclay cyclotron; we want to thank, in particular, R. Chaminade, A. Garin, R. Manse, and H. Poussard. We are indebted also to Dr. H. Sherif for his DWBA program with the FT term, to Dr. A. D. Hill for his coupled-channel program, and to W. S. Hall for his peak-stripping program. The visitors to Saclay greatly appreciate the hospitality of the Center. Two of us (A. G. B. and R. de S.) wish to acknowledge the financial support of NATO during part of this work.

[30] H. Sherif and R. de Swiniarski, Phys. Letters **28B**, 96 (1968).